Secondary Structure and Oligomerization Behavior of Equilibrium Unfolding Intermediates of the λ Cro Repressor†

Heinz Fabian,*,‡ Katja Fälber,‡ Klaus Gast,‡ Diane Reinstädler,§ Vladimir V. Rogov,||,⊥ Dieter Naumann,§ Dmitry F. Zamyatkin,|| and Vladimir V. Filimonov||

Max-Delbrück-Center for Molecular Medicine, Robert-Rössle-Strasse 10, D-13125 Berlin, Germany, Robert Koch-Institute, Nordufer 20, D-13353 Berlin, Germany, Institute of Protein Research, Russian Academy of Sciences, Pushchino, Moscow Region 142292, Russia, and J.W. Goethe University Frankfurt, Institute for Biophysical Chemistry, D-60439 Frankfurt, Germany

Received September 1, 1998; Revised Manuscript Received February 9, 1999

ABSTRACT: The thermal unfolding of the wild-type Cro repressor, its disulfide-bridged mutant Cro-V55C (with the Val-55 → Cys single amino acid substitution), and a CNBr-fragment $(13-66)_2$ of Cro-V55C was studied by Fourier transform infrared spectroscopy and dynamic light scattering. The combined approach reveals that thermal denaturation of Cro-WT and Cro-V55C proceeds in two steps through equilibrium unfolding intermediates. The first thermal transition of the Cro-V55C dimer involves the melting of the α-helices and the short β-strand localized in the N-terminal part of the molecule. This event is accompanied by the formation of tetramers, and also impacts on the hydrogen-bonding interactions of the C-terminal β-strands. The β-sheet formed by the C-terminal parts of each polypeptide chain is the major structural feature of the intermediate state of Cro-V55C and unfolds during a second thermal transition, which is accompanied by the dissociation of the tetramers. Cutting of 12 amino acids in the N-terminal region is sufficient to prevent the formation of α-helical structure in the CNBr-fragment of Cro-V55C, and to induce tetramerization already at room temperature. The tetramers may persist over a broad temperature range, and start to dissociate only upon thermal unfolding of the β-sheet structure formed by the C-terminal regions. The wild-type protein is a dimer at room temperature and at protein concentrations of 1.8−5.8 mg/mL. At lower concentrations, the dimers are stable until the onset of thermal unfolding, which is accompanied by the dissociation of the dimers into monomers. At higher protein concentrations, the unfolding is more complex and involves the formation of tetramers at intermediate temperatures. At these intermediate temperatures, the Cro-WT has lost all of its α-helical structure and also most of its native β-sheet structure. Upon further temperature increase, a tendency for an intermolecular association of the β-strands is observed, which may result in irreversible β-aggregation at high protein concentrations.

The information on non-native protein structures and, in particular, on folding intermediates is considered to be important for understanding protein folding processes. A major point of dispute is whether partly folded polypeptide chains are productive along the folding pathway, or whether they represent nonproductive misfolded forms (*1*, *2*). For experimental studies, stable species that can exist at equilibrium under conditions where the native state is destabilized are very attractive, because they permit one to reveal what these species look like and which forces are stabilizing these structures (*3*, *4*).

The Cro repressor of the λ phage, a small DNA-binding protein consisting of 66 amino acids, is one of these rare proteins which form equilibrium intermediates during unfolding. As far as known, this molecule is active only in its dimeric form (*5*). X-ray (*6*) and NMR[1] (*7*, *8*) structural analyses have shown that the dimer interface consists of a β-strand from the C-terminal part of each subunit, which pair to form an antiparallel β-ribbon, while the N-terminal parts comprising almost two-thirds of the whole molecule form small globular, predominantly α-helical, subdomains. Spectroscopic and calorimetric studies have suggested that the thermal unfolding of the wild-type Cro repressor (Cro-WT) at neutral pH and low protein concentration can be approximated by a two-state transition (*9*, *10*). More recently, a number of engineered Cro mutants which affect the stability and/or conformation of the protein were designed (*11*−*14*).

† This work was supported by INTAS Grant 93-007 and Deutsche Forschungsgemeinschaft Grant 436RUS113/360/0 to V.V.R. V.V.F. and D.F.Z. also acknowledge financial support from PECO Grant ERBCIPDCT940298. The work of H.F. and K.G. is also supported by grants from the Deutsche Forschungsgemeinschaft (Ga 175/12-1 and He 1318/20-1). K.F. acknowledges support from Graduierten Colleg 268 of the Deutsche Forschungsgemeinschaft.

* Author to whom correspondence should be addressed. Fax: 0049-30-94062548. E-mail: fabian@mdc-berlin.de.

‡ Max-Delbrück-Center for Molecular Medicine.

§ Robert Koch-Institute.

|| Russian Academy of Sciences.

⊥ J.W. Goethe University Frankfurt.

[1] Abbreviations: Cro-WT, wild-type Cro repressor; Cro-V55C, mutant with valine-55 replaced by cysteine; CNBr-fragment of CNBr-V55C, a S−S cross-linked fragment (residues 13−66) obtained by CNBr hydrolysis of the Cro-V55C mutant; CNBr, cyanogen bromide; FT-IR, Fourier transform infrared; DLS, dynamic light scattering; DSC, differential scanning calorimetry; NMR, nuclear magnetic resonance; CD, circular dichroism.

10.1021/bi982120d CCC: $18.00
Published on Web 04/06/1999

In one of these Cro mutants, with Val-55 replaced by Cys (Cro-V55C), a disulfide cross-link is spontaneously generated between the protein subunits (*12*). It was shown that this cross-link does not significantly perturb the structure, but that the disulfide bridge stabilizes the protein structure against thermal denaturation (*15*, *16*). Disulfide cross-linking also converts an apparently one-step melting of the wild-type protein into a clear two-step process (*17*). On the basis of calorimetric data, it was suggested that the heat denaturation of Cro-V55C starts with melting of the two globular N-terminal parts and ends with the unfolding of the β-sheet structure which is formed by the cross-linked C-terminal regions (*18*).

More recently, two of us have done extended differential scanning calorimetry (DSC) and circular dischroism (CD) spectroscopy studies of Cro-WT and Cro-V55C. The thermal denaturation of both proteins was found to be markedly concentration dependent, and the data suggested that in both cases unfolding occurs via a highly-populated intermediate state corresponding to a complex of the two partially unfolded Cro molecules (*19*). The unfolding model suggested by previous calorimetric studies is of interest for several reasons. It implies that an alternative partially ordered structure becomes more favorable than the native one at certain conditions, which must not necessarily be high temperature. Furthermore, this alternative conformation might be stabilized by an intermolecular association of β-strands at the expense of breaking down the globular arrangement of α-helices in a way which is phenomenologically very similar to the formation of amyloids (*20*, *21*) or other massive association phenomena of high physiological importance. However, in the case of Cro repressor molecules, the association is reversible and can be terminated at the level of oligomer formation, which allows its characterization by equilibrium methods.

In order to directly correlate changes in the secondary and tertiary structure of the Cro proteins with variations in their state of association, we have undertaken a combined Fourier transform infrared (FT-IR) spectroscopic and dynamic light scattering (DLS) study. FT-IR spectroscopy has emerged as a powerful technique for following changes in the secondary and tertiary structure of proteins under equilibrium and non-equilibrium conditions (*22*, *23*). DLS techniques, on the other hand, provide information concerning molecular mass and the hydrodynamic Stokes radius of the proteins in solution (*24*, *25*). Herein, the combined FT-IR and DLS approach permitted a detailed description of structural changes in Cro-WT, Cro-V55C, and in the CNBr-fragment of Cro-V55C upon thermal folding, and allowed characterization of the structural features of Cro unfolding intermediates.

MATERIALS AND METHODS

Proteins. Wild-type Cro-repressor and Cro-V55C were isolated and purified as described elsewhere (*26*). The CNBr-fragment was obtained by hydrolysis of Cro-V55C with CNBr and purified (*18*).

Infrared Spectroscopy. Infrared spectra were recorded on a Bruker IFS-66 FT-IR spectrometer equipped with a liquid nitrogen cooled mercury cadmium telluride detector and continuously purged with dry air. All samples were extensively dialized against water and lyophilized. Prior to the infrared experiments, the samples were dissolved in H_2O or D_2O containing 10 mM sodium cacodylate. Sample pH was adjusted to the required value with DCl or NAOD (HCl or NaOH for samples in H_2O); electrode readings were uncorrected for deuterium isotope effects. Protein solutions were placed between a pair of CaF_2 windows separated by a pathlength of 6 μm for H_2O samples or 45 μm for D_2O samples. For each sample, 1024 interferograms were coadded and Fourier-transformed employing a Happ−Genzel apodization function to generate a spectrum with a nominal resolution of 4 cm^{-1}. The sample temperature was controlled by means of a thermostated cell jacket. To obtain spectra at discrete temperatures, the protein solutions were heated in intervals of 5 °C. Spectra at these temperatures were recorded by equilibrating the sample for 5 min prior to data collection which itself took 6 min. Solvent specra were recorded under identical conditions and subtracted from the spectra of the proteins in the relevant solvent and at the corresponding temperatures. Minor spectral contributions from residual water vapor were eliminated using a set of water vapor spectra, as described earlier (*27*). The final unsmoothed protein spectra were used for further analysis. All illustrated spectra are shown after band-narrowing by Fourier self-deconvolution (*28*) to resolve overlapping infrared bands using a half-bandwidth of 16 cm^{-1} and a band-narrowing factor $k = 2.0$.

Light Scattering. Static and dynamic light scattering investigations were performed using an experimental setup which has been described previously (*29*). Briefly, an argon laser (LEXEL 3500) operating at the wavelength $\lambda = 514.5$ nm was used, and the scattered light was detected at an angle of 90°. The output laser power was in the range of 0.3−1.0 W depending upon the concentration of the protein samples. Derived from the solvent conditions used for the infrared experiments, the proteins were dissolved in H_2O containing 10 mM sodium cacodylate, and the sample pH was adjusted to 4.4 for Cro-V55C and its fragment and to 5.5 for the wild-type protein. To reduce dust or bubbles in the solutions, both the solvent and the protein solutions were filtered through 100 nm pore-size filters (Whatman, U.K.) located directly in front of the 100 μL flow-through light scattering cell (Hellma, Germany). Protein concentrations were measured photometrically in the rectangular light scattering cell and were calculated using UV extinction coefficients published elsewhere (*17*, *18*). The sample temperature was controlled by means of a thermostated cell jacket, and was changed in intervals of 5 or 10 °C. Data at the corresponding temperatures were recorded by equilibrating the sample for 5−10 min prior to data collection which itself took between 20 and 40 min.

For dynamic light scattering, homodyne time-autocorrelation functions of the scattered intenstiy, $G^{(2)}(\tau)$, were calculated by a 90-channel multibit multiple-τ correlator and then sent to an on-line-coupled PC for further data evaluation using the program CONTIN (*30*). The program CONTIN permitted calculation of the distribution function of translational diffusion coefficients, D, which were converted into apparent Stokes radii, $R_{S,app}$, via the Stokes−Einstein equation:

$$R_{S,app} = \frac{kT}{6\pi\eta_0 D} \quad (1)$$

where k is the Boltzmann constant, T the temperature in degrees kelvin, and η_0 the solvent viscosity. The latter parameter was determined using a Viscoboy viscosimeter (Lauda, Germany) and a DMA 58 digital density meter (Anton Paar KG, Austria). Typically, the distribution function obtained for protein solutions is characterized by a major peak yielding the diffusion coefficient of the protein molecules and sometimes a minor, well-separated peak, which indicates the presence of unavoidable dust and/or trace amounts of aggregated protein. If the protein molecules exist as monomers and small oligomers (e.g., dimers and tetramers), the major peak yields an average diffusion coefficient over these species, since a further deconvolution of this peak is in general not feasible.

During the evaluation of the static and the dynamic light scatting data, the concentration dependence of the measured quantities has to be taken into consideration. This can be described by a virial expansion (*31*). The dependence of the diffusion coefficients upon protein concentration is given via the equation:

$$D = D_0(1 + k_D c + ...) \quad (2)$$

k_D is the second diffusive virial coefficient which takes into account the interaction between protein molecules while c is the protein concentration. In the absence of strong interactions between protein molecules, a linear fit gives the diffusion coefficient at zero concentration (D_0). Otherwise, the situation is more complex, and then higher order terms must be included.

The concentration-dependent apparent molecular masses of the proteins were estimated from integrated light scattering experiments using benzene as intensity reference standard and a typical value of $dn/dc = 0.19$ mL/g for the refraction index increment of proteins. The weight-averaged molecular masses of the proteins, M_W, were determined via the equation:

$$(M_{W,app})^{-1} = (M_W)^{-1} + 2A_2c + ... \quad (3)$$

where A_2 is the second osmotic virial coefficient. Again, for more complex slopes, additionally higher order terms have to be used to get an appropriate fit. Here, it is important to get properly zero extrapolated quantites, while the concentration dependencies themselves will be discussed only qualitatively.

RESULTS

Infrared Studies. (A) Assignment of Infrared Bands. Figure 1shows representative deconvolved infrared spectra of Cro-V55C and the cross-linked CNBr-fragment in H_2O, in D_2O after an incubation period of 1 h at room temperature, and in D_2O after complete N^1H-N^2H exchange. In H_2O, the infrared spectra are dominated by the amide I band (C═O stretching vibration of all the amide groups) in the range 1620−1700 cm^{-1} and the amide II band. The protein backbone amide II band (primarily peptide N−H bending) centered near 1550 cm^{-1} in H_2O is shifted to 1450 cm^{-1} in N^1H-N^2H-exchanged proteins. Infrared bands that remain between 1500 and 1615 cm^{-1} after complete N^1H-N^2H exchange are entirely due to amino acid side chain absorptions: tyrosine (∼1515 and 1615 cm^{-1}), arginine (∼1586 and 1609 cm^{-1}), aspartate (∼1587 cm^{-1}), and glutamate (∼1580 cm^{-1}) (*32*). The spectrum of Cro-V55C obtained 1 h after exposure to D_2O shows that there is still considerable intensity retained in the amide II region at 1550 cm^{-1}. Such a behavior is typical of proteins whose backbone amide protons are incompletely exchanged (*33*) due to buried and/or strongly hydrogen-bonded amide N−H protons. Complete N^1H-N^2H exchange in Cro-V55C was only achieved by keeping the protein solution in D_2O for 30 min a few degrees below the denaturation temperature (i.e., 80 °C at pH 4). A similar resistance to backbone amide exchange has been reported for several other small proteins (*27*, *34*). The CNBr-fragment, on the other hand, exchanges significantly within 1 h of dissolving the lyophilized protein in D_2O, as indicated by the much stronger disappearance of the amide II band centered near 1550 cm^{-1} (Figure 1, right panel), indicating that the initial conformation of CNBr-V55C is less structured and/or more flexible than the intact cross-linked protein. In the range 1630−1660 cm^{-1}, the spectrum measured 1 h after exposure to D_2O is very similar to the spectrum obtained after thermal unfolding and cooling the sample down to room temperature (compare the middle and upper traces in Figure 1, right panel). The only detectable spectral difference between the partially and the fully exchanged CNBr-fragment concerns the band components at 1624−1626 and 1679−1684 cm^{-1}.

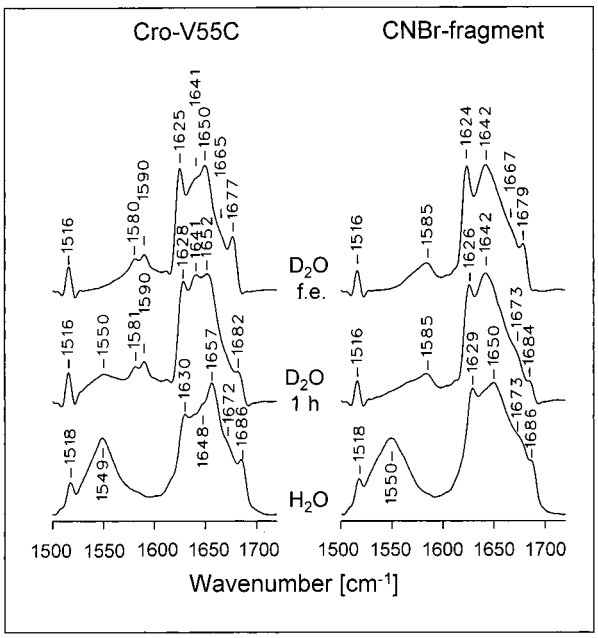

FIGURE 1: Infrared spectra of Cro-V55C (left panel) and its CNBr-fragment (right panel) in H_2O (bottom), in D_2O after an incubation period of 1 h (middle), and in D_2O after complete N^1H-N^2H exchange (top) at pH 4. All spectra are shown after Fourier self-deconvolution performed with the parameters given under Materials and Methods.

The deconvolved spectra of Cro-V55C reveal the presence of at least five individual band components in the amide I region. On the basis of established spectrum−structure correlations (*35*), the spectral changes observed after dissolving the proteins in D_2O, and a comparison with the infrared spectra of the CNBr-fragment, these five band components can be assigned to characteristic secondary structure elements. Thus, the amide I band at 1657 and 1650 cm^{-1} in H_2O and D_2O, respectively, can be assigned to

α-helical structures. This assignment is strongly supported by the lack of the corresponding band in the infrared spectrum of the CNBr-fragment, which is expected to be structureless in its N-terminal region (*18*). The band at 1625 cm^{-1} present in D_2O is assigned to the low-frequency component characteristic of antiparallel β-sheet structures (the corresponding band in H_2O is located at 1630 cm^{-1}), while the band at 1677 cm^{-1} (in D_2O) contains significant contributions from the high-frequency β-band. The appearance of a high-frequency band in the infrared spectra of β-sheet proteins is attributed to the formation of antiparallel β-strands, in which the close alignment of the polypeptide chains allows transition dipole coupling, which produces a splitting of the amide I mode (*36*). The occurrence of the characteristic β-structure features, at 1624 and 1679 cm^{-1}, in the spectrum of the CNBr-fragment indicates that its cross-linked C-terminal parts also form antiparallel β-strands. Furthermore, the band component at 1650 cm^{-1} in H_2O and 1642 cm^{-1} in D_2O, which shows a downshift soon after dissolution of the mutant V55C in D_2O, is assigned to irregular protein segments. Finally, turn structures in Cro-V55C are indicated by a shoulder centered near 1672 and 1665 cm^{-1} in H_2O and D_2O, respectively.

Because infrared spectra of proteins in heavy water have the advantage of a clear separation of side-chain absorptions from the protein backbone amide bands, all further measurements were carried out with D_2O solutions. This permitted us to follow conformational changes in the Cro repressor proteins by using peptide backbone amide I bands and specific side-chains bands as well separated and independent conformation-sensitive monitors.

(B) Thermal Stability and Unfolding Characteristics of the Cross-Linked Proteins. The experimental conditions for the measurements at different temperatures were selected such that heat denaturation was complete at the highest temperature available by the FT-IR setup. On the basis of our previous DSC studies, a pH near 4, low ionic strength, and a protein concentration of 13−16 mg/mL were chosen for the studies of Cro-V55C and its CNBr-fragment in order to decrease the stability of the intermediate state without decreasing its population during the FT-IR experiments.

Figure 2 shows typical infrared spectra of Cro-V55C recorded between 20 and 95 °C. In the amide I region, the spectra measured between 20 and 40 °C are similar to each other, indicating merely minor structural changes over this temperature range. On the other hand, the spectra measured at 40 and 50 °C are clearly different, demonstrating that major structural changes occur over this temperature range. This temperature range corresponds to the significant heat capacity absorption associated with the first DSC peak centered at 46 °C for Cro-V55C (DSC data not shown). In particular, the amide I band at 1650 cm^{-1}, which is assigned to α-helical structures, seems to disappear. In contrast, the loss of some intensity at 1625/1677 cm^{-1} indicates that only minor fractions of the native β-sheet structure of Cro-V55C unfold between 20 and 60 °C. The temperature-induced unfolding of proteins not only involves the melting of the various secondary structure elements but also leads to changes in the microenvironment of side-chain groups. A comparison of the spectra of Cro-V55C shown in Figure 2 reveals that the band-doublet at 1580 and 1590 cm^{-1} merges to a broad band centered at 1585 cm^{-1}. This suggests changes

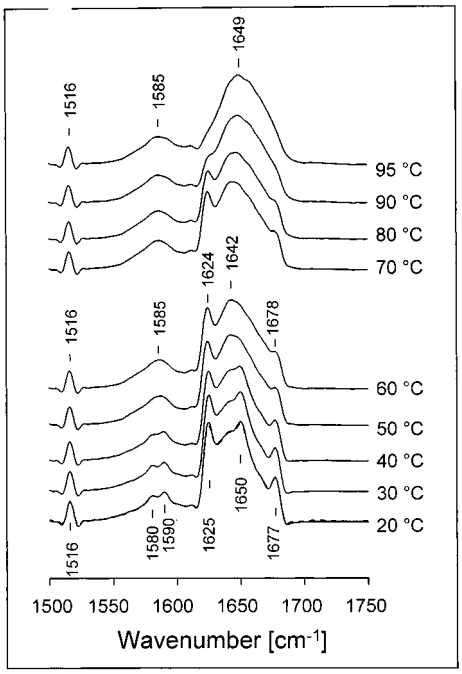

FIGURE 2: Infrared spectra (after Fourier self-deconvolution) of Cro-V55C in D_2O at pH 4 after complete N^1H-N^2H exchange at the indicated temperatures. Note that the spectra obtained at 20 °C before heating (solid line at 20 °C) and after cooling from 95 °C down to 20 °C (dashed line at 20 °C) are practically identical.

in the microenvironment of the carboxylate moiety of (some of) the amino acid side-chain groups of glutamate and aspartate in Cro-V55C between 20 and 60 °C. However, the assignment of the bands in the range 1570−1590 cm^{-1} due to carboxyl groups is only tentative at the moment because they are not observed in water and data on the symmetric bands are not available.

The spectra measured above 60 °C are dominated by a loss of the amide I band components at 1625 and 1677 cm^{-1}, which originate from antiparallel β-sheet structures. These spectral changes correspond to the second heat absorbance peak which is centered around 75 °C at our experimental conditions. The spectrum after thermal denaturation, at 95 °C, exhibits only a broad and nearly featureless amide I band contour centered at 1649 cm^{-1}. Such a contour is typical of predominantly irregular protein structures (*37*).

Infrared spectra of the CNBr-fragment were also measured at discrete temperatures between 20 and 95 °C. According to published DSC data, the melting curve of CNBr-V55C has only one peak of heat absorbance situated at temperatures similar to those of the second peak of the Cro-V55C thermogram (*18*), suggesting that the conformation of the CNBr-fragment might be similar to those of the Cro-V55C intermediate state. This suggestion is supported by the high similarity between the infrared spectrum of the fragment of Cro-V55C (top panel on the right side of Figure 1) and the spectrum of the intact protein obtained at 60 °C (middle trace in Figure 2).

To illustrate the structural changes occurring at low (between 20 and 60 °C) and high temperatures (between 60 and 95 °C), difference spectra obtained from spectra measured at the corresponding temperatures were calculated and are shown in Figure 3 for Cro-V55C (bottom panel) and for the CNBr-fragment (top panel). Remarkably, the spectral

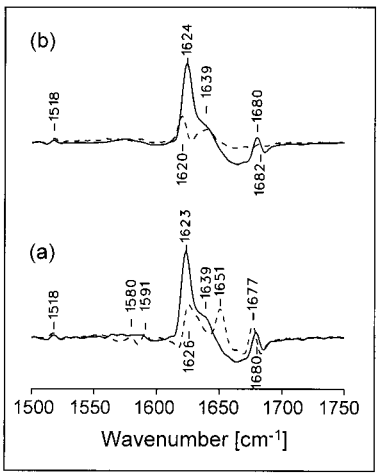

FIGURE 3: (a, bottom panel) Infrared difference spectra of Cro-V55C: (dashed line) spectrum measured at 20 °C minus spectrum measured at 60 °C; (solid line) spectrum measured at 60 °C minus spectrum measured at 95 °C. (b, top panel) Infrared difference spectra of the CNBr fragment: (dashed line) spectrum measured at 20 °C minus spectrum measured at 60 °C; (solid line) spectrum measured at 60 °C minus spectrum measured 95 °C. All difference spectra were obtained from the deconvolved spectra.

changes observed between 60 and 95 °C are very similar for both proteins (compare the solid lines in Figure 3, bottom and top panels), suggesting comparable structural changes over this temperature range. Only a minor difference is indicated by the shoulder at 1639 cm^{-1}, which is more pronounced in the corresponding difference spectrum of Cro-V55C. The spectral changes observed between 20 and 60 °C, however, are obviously quite different for both proteins. Most striking, the positive difference peak at 1651 cm^{-1}, which is assigned to α-helical structures, is absent in the spectrum of the CNBr-fragment, clearly indicating the lack of α-helical structures in the fragment. Furthermore, changes in the region of the β-sheet "marker" bands are much less pronounced for the CNBr-fragment and different in frequency for both proteins. In the case of Cro-V55C, the spectral changes in this region also clearly differ from the corresponding changes observed above 70 °C. Striking are differences in splitting of the low- and high-frequency β-sheet band components (compare the dashed and solid lines in Figure 3a) and the presence of negative features for the low-temperature transition. This indicates not only a loss of intensity but also changes in frequency of the corresponding bands upon temperature increase from 20 to 60 °C. The small increase in band splitting by 2−3 cm^{-1} suggests that the remaining β-sheet structure in the intermediate state of Cro-V55C is experiencing a slightly stronger hydrogen bonding in comparison to the native state. This indicates that unfolding of the three α-helices in the N-terminal region and disruption of parts of the native β-sheet structure are accompanied by a reorganization of the remaining β-sheet.

The positive band at 1620 cm^{-1} (dashed line in Figure 3b) indicates that some β-structure in the fragment unfolds between 20 and 60 °C. The second positive band centered at 1639 cm^{-1} suggests that additional spectral band components disappear during the low-temperature transition. The assignment of these latter features is complicated by the fact that β-turn (*35*) or even α-helices with additional hydrogen bonding of the solvent-accessible backbone C═O groups to water (*38*) may exhibit an infrared band near 1639 cm^{-1}. As mentioned before, a shoulder at 1639 cm^{-1} is also observed in the difference spectrum of Cro-V55C betwen 60 and 95 °C, but much less pronounced in the corresponding difference spectrum of the fragment. Thus, it seems reasonable to assume that at least parts of the structure(s), which give(s) rise to the spectral feature at 1639 cm^{-1} and which melt(s) between 20 and 60 °C in the fragment, is (are) more stable in Cro-V55C. Moreover, spectral changes in the region between 1560 and 1590 cm^{-1} are only observed for Cro-V55C. Because of the tentative character of their assignment, these spectral changes cannot be interpreted at the moment.

(C) Thermal Unfolding of the Wild-Type Protein. Finally, we have also studied temperature-induced spectral changes in the wild-type Cro repressor at pH 5.0 and at a protein concentration of approximately 10 mg/mL. The higher pH value was chosen because DSC studies indicated that the native structure of Cro-WT is much less stable than that of the cross-linked mutant and that the stability of the intermediate state has a much stronger dependence upon the protein concentration. Therefore, in a thermodynamic sense, pH 5.0 for Cro-WT is a sort of equivalent to pH 4.0 for Cro-V55C. The analysis of DSC curves of Cro-WT obtained at this pH and low ionic strength revealed two heat absorption peaks on the thermogram even at a relatively low protein concentration of 0.21 mM. The amplitudes of both peaks, however, were found to be smaller than those observed for Cro-V55C (*19*). Despite the bimodality of unfolding, the population of the intermediate state was very small at the concentration of 0.21 mM, and the unfolded state was more populated than the intermediate one at any temperature. To get the intermediate state really populated, it was necessary to increase the protein concentration up to 0.68 mM (10.0 mg/mL). Further concentration increase, however, resulted in disadvantageous movement of the first peak toward lower temperatures and of the second one to higher temperatures. Therefore, the choice of optimal protein concentrations for the FT-IR experiments was very important.

The infrared spectra of Cro-WT in H_2O, after 1 h in D_2O, and after complete N^1H-N^2H exchange in D_2O are shown in Figure 4, left side. Comparison of the spectra of the wild-type protein obtained in H_2O and in D_2O after complete H/D exchange with the corresponding spectra of Cro-V55C (see Figure 1, left panel) reveals very similar spectra, proving that the basic Cro-fold is very similar in the Cro-WT and Cro-V55C proteins. The spectra of these proteins measured after an incubation period of 1 h in D_2O, however, are clearly different. The corresponding spectrum of Cro-WT is already almost identical to the spectrum measured after keeping the wild-type protein in D_2O at high temperatures (compare the middle and top panels in Figure 4, left side). This shows that the wild-type protein spontaneously exchanges almost all of its amide protons within 1 h after dissolving the lyophilized protein in D_2O.

The infrared spectra of the Cro-WT were also measured between 20 and 95 °C in intervals of 5 °C. Spectra obtained for the folded state (20 °C), at intermediate temperature (60 °C), and at high temperature (95 °C) are shown in Figure 4, right panel. The inset in the upper right corner shows difference spectra, which clearly illustrate the spectral changes that occur between 20 and 60 °C (dashed line) and between 60 and 95 °C (solid line). Both presentations show

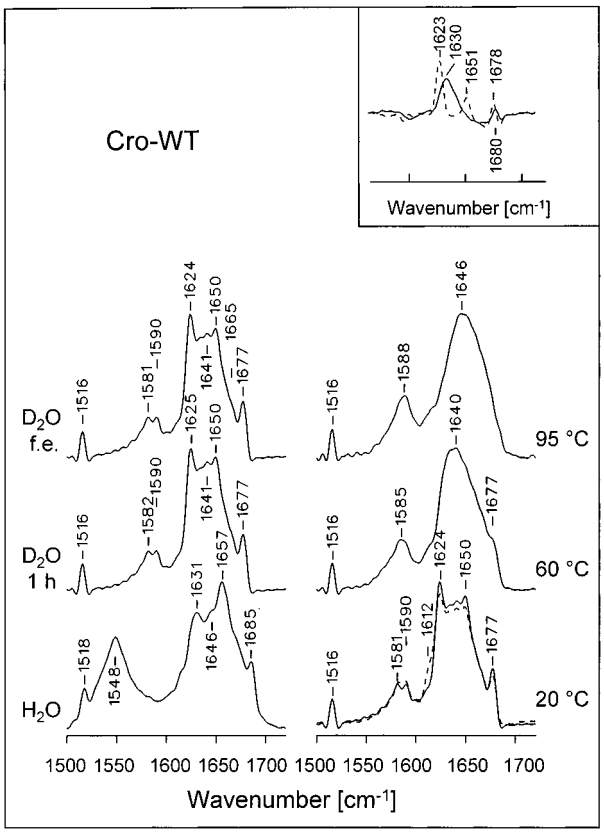

FIGURE 4: Infrared spectra of the wild-type Cro repressor in H_2O (bottom), in D_2O after an incubation period of 1 h (middle), and in D_2O after complete exchange (top) at pH 5.6 (left panel). Infrared spectra of the wild-type Cro repressor in D_2O at the indicated temperatures (right panel). The dashed line shows the spectrum obtained after cooling from 95 °C down to 20 °C. All spectra are shown after Fourier self-deconvolution. Inset: Infrared difference spectra obtained from the deconvolved spectra of Cro-WT; (dashed line) spectrum measured at 20 °C minus spectrum measured at 60 °C; (solid line) spectrum measured at 60 °C minus spectrum measured at 95 °C.

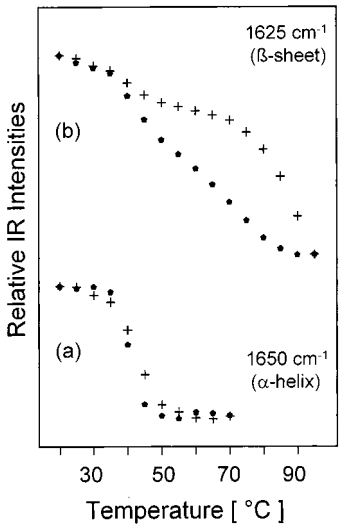

FIGURE 5: Temperature dependence of the peak height intensity of the amide I band at 1650 cm^{-1} (α-helix; panel a) and at 1625 cm^{-1} (β-sheet; panel b) for Cro-WT (●) and for Cro-V55C (+). Intensities were normalized with respect to band intensities obtained at low and high temperatures for the corresponding amide I marker bands.

that the band diagnostic of α-helical structures at 1650/51 cm^{-1} disappears between 20 and 60 °C, indicating the unfolding of three α-helices. The spectral features of the β-bands, however, are at clear variance with our results obtained for the cross-linked protein. Infrared bands at 1624 and 1677 cm^{-1} are almost completely absent in the original spectrum of the wild-type protein 60 °C (middle trace in Figure 4, right side), while intense positive bands at 1623 and 1678 cm^{-1} are observed in the corresponding difference spectrum (inset, dashed line). This indicates that the wild-type protein in contrast to its cross-linked variant has lost most of its canonical β-structure at 60 °C. The spectral changes observed at higher temperatures also indicate the unfolding of any kind of β-sheet structure in the wild-type protein. The difference spectroscopic features (e.g., a broad low-frequency component centered at 1630 cm^{-1}), however, resemble neither those of the melting of the well-defined β-sheet structure in the native protein between 20 and 60 °C (a sharp band at 1623 cm^{-1}) nor those of the melting of the β-sheet structure in the C-terminal region of Cro-V55C between 60 and 95 °C (a sharp band at 1623 cm^{-1}; Figure 3a). A partially unfolded state containing a well-structured β-sheet domain, such as demonstrated by the infrared data for Cro-V55C, is not suggested for the wild-type protein under our experimental conditions. The spectrum at 95 °C exhibits only a broad, nearly featureless amide I band contour, suggesting a predominantly irregular protein structure under this condition. The spectrum obtained after cooling the protein sample from 95 °C down to 20 °C was not identical to the spectrum before heating (compare the solid and dashed lines on the bottom in Figure 4, right panel). This indicates that the thermal unfolding of the Cro-WT was not reversible. The appearance of a shoulder near 1612 cm^{-1} indicates the presence of intermolecular β-aggregates in the sample after thermal denaturation. The tendency for β-aggregation was found to vary depending upon the experimental conditions. When collecting infrared spectra along a linear temperature gradient, which in our case requires relatively long times for data acquisition, the β-aggregation "marker" band near 1612 cm^{-1} was already observed above 85 °C (data not shown). This is in contrast to corresponding measurements of Cro-V55C and its CNBr-fragment, where no indications for intermolecular β-aggregation were observed.

Differences in the unfolding characteristics of the wild-type Cro-repressor and its variant Cro-V55C can also be seen by comparison of the intensity/temperature plots for the amide I band components at 1650 (α-helix) and 1624/25 cm^{-1} (β-sheet). A comparison of the intensity changes at 1650 cm^{-1} (Figure 5a) reveals a broader transition profile for Cro-V55C, suggesting a slightly lower cooperativity of the unfolding of the three α-helices in Cro-V55C than in Cro-WT under our experimental conditions. The transition profiles derived from the temperature dependence of the β-band at 1625 cm^{-1} (Figure 5b) are very different for both proteins. They clearly indicate that a significant amount of β-sheet structure is still present in Cro-V55C at intermediate temperatures, but not in the wild-type protein. The overlapping of changes in intensity with changes in frequency, in particular for the Cro-V55C variant in the temperature range 20−60 °C as described before, creates some problems in the quantitative estimation of the numbers of hydrogen bonds

involved. Qualitatively, the loss of band intensity at 1625 cm^{-1} indicates that only between 25 and 33% of the total β-sheet structure of Cro-V55C unfolds between 20 and 60 °C. Assuming that the β-sheets in Cro-V55C are composed of the same residues as in the wild-type protein (*8*), then these are residues 3−6, 40−44, and 50−55. Because the first thermal transition of Cro-V55C involves the unfolding of all the α-helices in the N-terminal part of the molecule, it is very likely that this also causes the short N-terminal β-strand (residues 3−6) to detach itself from the β-sheet. This corresponds to 27% of the total number of residues in the β-ribbon of the Cro repressor, which would be in good agreement with the 25−33% derived from intensity losses of the β-band at 1625 cm^{-1}. This suggests that at intermediate temperatures not only the intermolecular β-sheet domain formed by the C-terminal parts of each polypeptide chain but likely also the β-strand composed of residues 40−44 still exists.

Dynamic Light Scattering Studies. The marked concentration dependence of the thermal denaturation of the Cro-repressor proteins previously observed during calorimetric studies (*19*) suggested that protein unfolding may also involve protein association. In order to directly monitor changes in molecular size and variations in the state of association, we have also carried out dynamic light scattering experiments on Cro-WT, Cro-V55C, and the CNBr-fragment of Cro-V55C at experimental conditions comparable to those applied for the FTIR studies described before. DLS measurements at different temperature revealed a complex interplay between changes in the molecular dimensions upon unfolding, molecular association, and changes in the molecular interactions. In order to separate the different effects as well as possible, the DLS data will be presented in the following way. First, the state of the proteins at 20 °C is characterized in terms of the weight-averaged molecular mass M_W, the diffusion coefficient D, or the corresponding Stokes radius R_S. Second, the concentration dependence of the diffusion coefficients of Cro-WT and Cro-V55C is presented at characteristic temperatures. Finally, the temperature-induced changes in normalized scattering intensity are discussed for each protein at selected concentrations.

Molecular Mass M_W, Diffusion Coefficients D, and Stokes Radii R_S of the Cro Proteins. The molecular masses of the three proteins at room temperature were estimated in order to check whether the folded states of the proteins can be characterized as monomer, dimer, or higher oligomers. For this purpose, the integrated light scattering intensities at 20 °C were measured at different concentrations of Cro-WT (1.8−5.8 mg/mL), of Cro-V55C (2.2−12.3 mg/mL), and of the CNBr-fragment of Cro-V55C (2.0−11.9 mg/mL). The weight-averaged molecular masses of the three proteins were estimated via eq 3 by extrapolation to zero concentration. For Cro-WT and Cro-V55C, the concentration dependence of $1/M_{app}$ was weak, and a linear extrapolation was adequate throughout the entire concentration range studied. For the CNBr-fragment, however, a clear deviation from linearity was observed, whereby a positive slope of $1/M_{app}$ versus c indicated remarkable repulsive intermolecular interactions (data not shown). A comparison of the experimentally estimated molecular masses (Table 1) with those calculated from the amino acid composition of a single polypeptide chain, 7.4 kDa for Cro-WT and Cro-V55C and 5.9 kDa for Cro-CNBr, suggests a folded state dominated by dimers for the Cro-WT and the Cro-V55C protein, but a tetrameric state for the CNBr-fragment.

Table 1: Stokes Radii and Molecular Masses of Cro-WT, Cro-V55C, and CNBr-Fragment in H_2O Containing 10 mM Sodium Cacodylate at 20 °C

	Cro-WT pH 5.5	Cro-V55C pH 4.4	CNBr-fragment pH 4.4
Stokes radius (nm)	2.10 ± 0.03	1.94 ± 0.02	2.61 ± 0.04
molecular mass (kDa)	14.6 ± 1.5	13.4 ± 1.3	23.4 ± 2.3

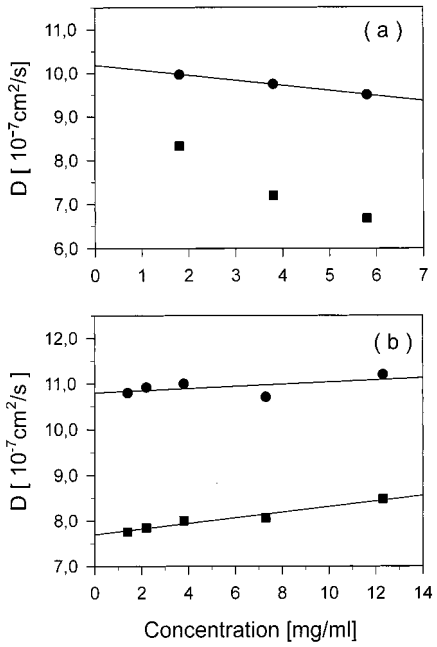

FIGURE 6: Concentration dependence of the diffusion coefficient D of (a) the wild-type Cro-repressor at 20 (●) and 55 °C (■) and (b) Cro-V55C at 20 (●) and 60 °C (■).

Figure 6 shows the concentration dependence of the diffusion coefficient of Cro-WT and of Cro-V55C. At 20 °C (circles), only moderate concentration dependence but of different sign is observed. The diffusion coefficient of the wild-type protein was found to decrease slightly upon concentration increase, suggesting an attractive interaction of predominantly dimers. The slightly positive slope for Cro-V55C hints at prevalent repulsive interactions. Similar, but somewhat stronger repulsive interactions were observed in the case of the tetramer-forming CNBr-fragment (data not shown). The Stokes radii of the three proteins at 20 °C obtained from the diffusion coefficients extrapolated to zero protein concentration are given in Table 1. The Stokes radius of Cro-V55C (1.94 nm) is slightly smaller than that of Cro-WT (2.10 nm), suggesting that the covalent dimer is more compact and/or more sphere-like than the dimer of the wild-type protein. The Stokes radius of the CNBr-fragment (2.61 nm) exceeds that of Cro-V55C by a factor of 1.32. Taking into account that the Stokes radius of a dimer of two spherical subunits is 1.39 times greater than that of the isolated subunits (*39*), a factor somewhat smaller than 1.39 can be expected because the fragment is lacking about 20% of the amino acid residues of Cro-V55C. This further supports the view that the CNBr-fragment of Cro-V55C exists as a tetramer at 20 °C.

The concentration dependencies change in a different manner at elevated temperature. At 55 °C, a drastic decrease in the diffusion coefficient of Cro-WT upon increasing the protein concentration was observed (Figure 6a, squares). This indicates an interplay between attractive interactions and molecular association, whereby the latter factor dominates. The existing concentration-dependent association makes an extrapolation to zero protein concentration meaningless. The concentration dependence is consistent with the existence of a mixture of dimers and tetramers within the investigated concentration range. At the highest protein concentration measured, an onset of irreversible aggregation of Cro-WT was observed at temperatures above 70 °C.

The lack of intermolecular irreversible aggregation of Cro-V55C and its CNBr-fragment at very high protein concentrations and high temperatures observed during the FTIR studies prompted us to carry out DLS experiments of these cross-linked proteins over a wider range of experimental conditions than applied for the wild-type protein. The concentration dependence of the diffusion coefficient of Cro-V55C at 60 °C (the equilibrium intermediate) exhibits a slightly steeper positive slope than at 20 °C (Figure 6b), suggesting a small increase in the already existing repulsive intermolecular interactions at the higher temperature. Furthermore, the diffusion coefficient changes in a linear manner as a function of protein concentration. This shows that the association state of Cro-V55C at 60 °C is concentration-independent under our experimental conditions. The fact that the diffusion coefficient extrapolated to zero protein concentration at 60 °C is smaller by a factor of 1.4 when compared to the corresponding value at 20 °C indicates a predominantly tetrameric state at the higher temperature.

Changes in the oligomerization behavior of Cro-WT, of Cro-V55C, and of its CNBr-fragment were directly measured by monitoring the normalized scattering intensity of the proteins at different temperatures and at different protein concentrations. Selected intensity/temperature plots are shown in Figure 7. From the same type of experiments, the Stokes radii were estimated. Changes in the latter parameter result from variations in the state of association and from unfolding of the polypeptide chain, and, thus, their interpretation is more complex. In the following, the Stokes radii will be discussed only in particular cases.

Thermal Unfolding of Cro-V55C. Figure 7a shows the temperature-induced changes in the normalized scattering intensity for Cro-V55C at two protein concentrations. At the lower protein concentration of 2.2 mg/mL (squares), there are practically no changes between 20 and 40 °C. Between 40 and 50 °C, there is a strong increase in intensity, demonstrating that the oligomerization state changes drastically over this temperature range. At approximately 5 times higher protein concentration, the temperature-induced changes (circles) begin earlier, and the transition profile is slightly broader. This suggests that the formation of larger oligomers, preferentially tetramers, depends upon temperature and protein concentration. At temperatures near 60 °C, the equilibrium is strongly shifted toward tetramers, and tetramers are predominantly present over the entire concentration range used in our experiments. Interestingly, the transition profile of the scattering intensity at a protein concentration of 12.3 mg/mL is very similar to the profile derived from intensity changes of the infrared band at 1650 cm^{-1} (Figure 5a), which was used to monitor the disruption of α-helical structures in Cro-V55C. The unfolding of secondary structure in the N-terminal region of Cro-V55C is obviously a precondition for its capability to form tetramers. Upon thermal denaturation, these tetramers dissociate again into dimers, as indicated by the strong decrease in intensity above 70 °C. It is puzzling that the increase in normalized scattering intensity upon temperature increase is lower at the higher protein concentration. This is due to repulsive forces between the partially unfolded polypeptide chains in the tetrameric state, leading to a remarkable concentration dependence of the scattering intensity as discussed before. This will result in smaller values of the normalized scattering intensity at higher protein concentrations, such as observed herein for Cro-V55C between 50 and 70 °C.

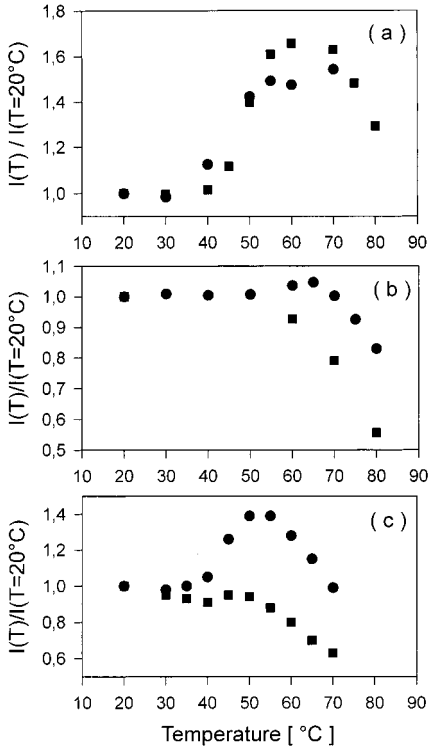

FIGURE 7: Temperature dependence of the normalized scattering intensities of (a) Cro-V55C: (■) 2.2 and (●) 12.3 mg/mL; (b) CNBr-fragment: (■) 2.0 and (●) 11.9 mg/mL; and (c) Cro-WT: (■) 1.8 and (●) 5.8 mg/mL.

Thermal Unfolding of the CNBr-Fragment. Figure 7b shows the temperature-dependent changes in normalized scattering intensity of the CNBr-fragment of low and high protein concentrations. The lack of changes between 20 and 50 °C indicates that the tetramers observed at ambient temperature exist over a wide temperature range. A strong decrease in the scattering intensity is only observed when the temperature approaches 80 °C. This decrease is more pronounced at the lower concentration (squares), and reflects a concentration-dependent dissociation of tetramers into dimers. This dissociation process led to only minor changes in the apparent Stokes radii (data not shown). A decrease in R_S, which could be expected due to the dissociation of tetramers, was obviously compensated by the expansion of the individual CNBr-fragment dimers as a consequence of unfolding.

Thermal Unfolding of Cro-WT. The temperature-induced changes in normalized scattering intensities of the Cro-WT

protein reveal a strong concentration dependence (Figure 7c). At a concentration of 1.8 mg/mL, the normalized intensity (squares) remains nearly constant between 20 and 50 °C. At the same time, the apparent Stokes radius increases between 40 and 50 °C (data not shown). This suggests an expansion of the protein molecules due to unfolding without the formation of tetramers. The decrease of the normalized scattering intensity above 50 °C indicates the dissociation of the dimers into unfolded monomeric polypeptide chains. Obviously, the interactions between the noncovalently linked β-sheets of the two polypeptide chains of the wild-type protein, which are necessary for the formation of the dimers, no longer exist at high temperatures. An only 3-times increase in protein concentration drastically impacts on the unfolding of the Cro-WT. The 40% increase in normalized intensity between 35 and 55 °C (Figure 7c, circles) indicates the formation of oligomers at intermediate temperatures. The loss of intensity above 55 °C suggests that these associates again dissociate at higher temperatures. At intermediate temperatures, there is obviously a mixture of tetramers and dimers, and its ratio depends upon the protein concentration; the higher the protein concentration, the more populated is the tetrameric state.

DISCUSSION

Recent calorimetric experiments suggested that unfolding of the Cro repressor and its mutants occur via intermediate states whose equilibrium population strongly depends upon the protein concentration. It was argued that the intermediate states are stabilized by association (tetramerization) of the partially unfolded polypeptide chains (*19*). The infrared spectroscopic and dynamic light scattering data obtained in this study provide detailed information on temperature-induced structural changes in Cro repressor proteins and on their association behavior.

The FT-IR spectra of the native states of Cro-WT and of Cro-V55C obtained after complete H−D exchange show a high degree of similarity. In particular, all five diagnostic infrared bands characteristic of a specific secondary structure indicate that the characteristic Cro-fold is maintained in both proteins. On the other hand, the protons within the native Cro-WT structure were found to exchange rather easily, whereas the Cro-V55C structure revealed a pronounced resistance to backbone amide exchange. Thus, although the secondary structures of both Cro-folds are very similar, the wild-type protein must be much more flexible. The higher rigidity of the structure of Cro-V55C derived from FT-IR studies herein is in full agreement with earlier NMR observations (*15, 16*).

The infrared spectra of Cro-WT and Cro-V55C clearly demonstrate the unfolding of α-helical structures in both proteins at intermediate temperatures, but at the same time characteristic differences regarding the β-structures present are detected under these conditions. First, the infrared bands at 1624 and 1677 cm^{-1} assigned to antiparallel β-sheet structures are much less intense, if present at all, in the spectra of Cro-WT. This indicates that, in contrast to Cro-V55C, Cro-WT has already lost most of its canonical β-sheet structure at intermediate temperatures. Second, different positions and shapes of the β-structure features in the difference spectra of the wild-type protein below and above 65 °C (a sharp band at 1623 cm^{-1} below 60 °C versus a broad band centered at 1630 cm^{-1} above 70 °C) suggest distinct differences in the hydrogen-bonding pattern of the amide C═O groups in the corresponding β-type structures. It is generally accepted that the weaker the hydrogen bond involving the amide C═O, the higher the amide I absorption appears (*35*). Using this empirical approach, the high amide I feature at 1630 cm^{-1} in the difference spectra of the Cro-WT points to relatively weak hydrogen-bonding interactions of the amide C═O groups involved in the β-type structures present in the wild-type protein above 65 °C. This situation, however, changes drastically if the protein is kept isothermally at intermediate temperatures for longer time periods. Under these conditions, intermolecular aggregates, indicated by the corresponding infrared "marker" band at 1612 cm^{-1}, are accumulating. At the moment, the β-type structures present in the wild-type Cro-repressor above 65 °C are not well described, but they certainly neither resemble the well-defined β-sheet structure in the native protein nor resemble the β-structure formed by the C-terminal parts in Cro-V55C at intermediate temperatures. Dynamic light scattering data indicate a primarily tetrameric state of Cro-WT near 65 °C and at a protein concentration of 5.8 mg/mL, which is approximately 2-fold lower that those applied for the infrared studies. In addition, a tendency for irreversible aggregation of the wild-type protein above 70 °C was observed. Interestingly, a 3-fold decrease in protein concentration was found to have a dramatic impact on the thermal unfolding of Cro-WT. At a concentration of 1.8 mg/mL, its unfolding proceeds without formation of tetramers. Furthermore, the disruption of the secondary structure above 40 °C is accompanied by the dissociation of dimers into unfolded monomeric molecules.

In contrast to the wild-type protein, a well-defined equilibrium intermediate was observed for the cross-linked Cro-V55C variant. This partially unfolded intermediate state of Cro-V55C is highly populated near 60 °C and contains a well-structured intermolecular β-sheet domain formed by the C-terminal parts of each polypeptide chain and, in contrast to temperatures between 20 and 50 °C, is a tetramer. Within the concentration range of 2.2−12.3 mg/mL used for the DLS studies, the state of association near 60 °C was found to be concentration-independent. During thermal denaturation above 70 °C, the tetramers start to dissociate again into dimers. Furthermore, the infrared spectra clearly revealed that unfolding of the structure in the N-terminal parts of the dimer between 20 and 60 °C also leads to distortions in β-strands in the cross-linked C-terminal regions which, however, essentially remain intact until temperatures near 60 °C. In addition, the close correlation between temperature-induced changes in light scattering parameters on the one hand and in secondary structure on the other hand indicates that the unfolding of the particular secondary structure in the N-terminal regions of Cro-V55C is a precondition for the tetramerization process. If the N-terminal regions are unable to form a defined secondary structure, such as in the CNBr-fragment of Cro-V55C, tetramerization takes place already at room temperature. These tetramers may persist over a wide temperature range, and start to dissociate into dimers only upon thermal unfolding of the structure formed by the C-terminal parts of the Cro-V55C fragment.

The present infrared spectroscopic and dynamic light scattering data do not provide details with respect to the nature of the interactions which stabilize the polypeptide chains in the tetrameric state. An answer can probably be obtained only after solving the structure of the intermediate state by NMR. For such an analysis, the CNBr-fragment of Cro-V55C, which is a tetramer already at ambient temperatures, might be a promising candidate.

Our further studies will concentrate on the kinetics of unfolding/refolding of the Cro repressor proteins by time-resolved FTIR spectroscopy, applying recently developed FTIR methodologies (*23*). From these experiments, we expect insights into the role of the tetrameric state on the folding pathway of the Cro repressor protein.

REFERENCES

1. Privalov, P. L. (1996) *J. Mol. Biol. 258*, 707−725.
2. Baldwin, R. L. (1997) *Nat. Struct. Biol. 4*, 965−966.
3. Kuwajima, K. (1989) *Proteins: Struct., Funct., Genet. 6*, 87−103.
4. Dobson, C. M. (1992) *Curr. Opin. Struct. Biol. 2*, 6−12.
5. Johnson, A., Meyer, B. J., and Ptashne, M. (1978) *Proc. Natl. Acad. Sci. U.S.A. 75*, 1783−1787.
6. Anderson, W. F., Ohlendorf, D. H., Takeda, Y., and Mathews, B. W. (1981) *Nature 290*, 754−758.
7. Weber, P. L., Wemmer, D. E., and Reid, B. R. (1985) *Biochemistry 24*, 4553−4562.
8. Matsuo, H., Shirakawa, M., and Kyogoku, Y. (1995) *J. Mol. Biol. 254*, 668−680.
9. Bolotina, I. A., Kurochkin, A. V., and Kirpichnikov, M. P. (1993) *FEBS Lett. 155*, 291−294.
10. Pakula, A. A., and Sauer, R. T. (1989) *Proteins: Struct., Funct., Genet. 5*, 202−210.
11. Mossing, M. C., and Sauer, R. T. (1990) *Science 250*, 1712−1715.
12. Hubbard, A. J., Bracco, L. P., Eisenbeis, S. J., Gayle, R. B., Beaton, G., and Caruthers, M. H. (1990) *Biochemistry 29*, 9241−9249.
13. Albright, R. A., Mossing, M. C., and Mathews, B. W. (1996) *Biochemistry 35*, 735−742.
14. Mollah, A. K. M. M., Alema, M. A., Albright, R. A., and Mossing, M. C. (1996) *Biochemistry 35*, 743−748.
15. Shirakawa, M., Hiroshi, M., and Kyogoku, Y. (1991) *Protein Eng. 4*, 545−552.
16. Baleja, J. D., and Sykes, B. D. (1994) *Biochem. Cell Biol. 72*, 95−108.
17. Gitelson, G. I., Griko, Y. V., Kurochkin, A. V., Rogov, V. V., Kutychenko, V. P., Kirpichnikov, M. P., and Privalov, P. L. (1991) *FEBS Lett. 289*, 201−204.
18. Griko, Y. V., Rogov, V. V., and Privalov, P. L. (1992) *Biochemistry 31*, 12701−12705.
19. Filimonov, V. V., and Rogov, V. V. (1996) *J. Mol. Biol. 255*, 767−777.
20. Harrison, P. M., Bamborough, P., Daggett, V., Prusiner, S. B., and Cohen, F. E. (1997) *Curr. Opin. Struct. Biol. 7*, 53−59.
21. Kelly, L. W. (1998) *Curr. Opin. Struct. Biol. 8*, 101−106.
22. Fabian, H., Schultz, C., Backmann, J., Hahn, U., Saenger, W., Mantsch, H. H., and Naumann, D. (1994) *Biochemistry 33*, 10725−10730.
23. Reinstädler, D., Fabian, H., Backmann, J., and Naumann, D. (1996) *Biochemistry 35*, 15822−15830.
24. Gast, K., Damaschun, G., Damaschun, H., Misselwitz, R., and Zirwer, D. (1993) *Biochemistry 32*, 7747−7752.
25. Gast, K., Nöppert, A., Müller-Frohne, M., Zirwer, D., and Damaschun, G. (1997) *Eur. Biophys. J. 25*, 211−219.
26. Rogov, V. V., and Griko, Yu. V. (1993) *Mol. Biol. (USSR) 27*, 798−804.
27. Fabian, H., Schultz, C., Naumann, D., Landt, O., Hahn, U., and Saenger, W. (1993) *J. Mol. Biol. 232*, 967−981.
28. Mantsch, H. H., Moffatt, D. J., and Casal, H. L. (1988) *J. Mol. Struct. 173*, 285−298.
29. Gast, K., Damaschun, G., Misselwitz, R., and Zirwer, D. (1992) *Eur. Biophys. J. 21*, 357−362.
30. Provencher, S. W. (1982) *Comp. Phys. Commun. 27*, 229−242.
31. Schmidt, M. (1993) in *Dynamic Light Scattering. The method and some applications* (Brown, W., Ed.) pp 372−406, Clarendon Press, Oxford.
32. Chirgadze, Y. N., Fedorov, O. V., and Trushina, N. P. (1975) *Biopolymers 14*, 679−694.
33. Blout, E. R., de Loze, C., and Asadourian, A. (1961) *J. Am. Chem. Soc. 83*, 1895−1900.
34. Backmann, J., Schultz, C., Fabian, H., Hahn, U., Saenger, W., and Naumann, D. (1996) *Proteins: Struct., Funct., Genet. 24*, 379−387.
35. Jackson, M., and Mantsch, H. H. (1995) *Crit. Rev. Biochem. Mol. Biol. 30*, 95−120.
36. Krimm, S., and Bandekar, J. (1986) *Adv. Protein Chem. 38*, 181−364.
37. Fabian, H., and Mantsch, H. H. (1995) *Biochemistry 34*, 13651−13655.
38. Reisdorf, W. C., and Krimm, S. (1996) *Biochemistry 35*, 1383−1386.
39. Garcia Bernal, J. M., and Garcia de la Torre, J. (1981) *Biopolymers 20*, 129−139.

BI982120D